Morphometric development of the human fetal cerebellum during the early second trimester

Feifei Xu[a,c,1], **Xinting Ge**[b,c,1], **Yonggang Shi**[c], **Zhonghe Zhang**[a,d], **Yuchun Tang**[a], **Xiangtao Lin**[a,d], **Gaojun Teng**[e], **Fengchao Zang**[e], **Nuonan Gao**[f], **Haihong Liu**[b], **Arthur W. Toga**[c], **Shuwei Liu**[a,*]

[a]Research Center for Sectional and Imaging Anatomy, Shandong University Cheeloo College of Medicine, 250012, Jinan, Shandong, China

[b]Department of Medical Imaging, Xuzhou Medical University, 221004, Xuzhou, Jiangsu, China

[c]Laboratory of Neuro Imaging (LONI), USC Stevens Neuroimaging and Informatics Institute, Keck School of Medicine of University of Southern California, Los Angeles, CA, 90033, USA

[d]Department of Medical Imaging, Provincial Hospital Affiliated to Shandong University, 250021, Jinan, Shandong, China

[e]Department of Radiology, Zhong Da Hospital, Southeast University School of Clinical Medicine, 210009, Nanjing, Jiangsu, China

[f]Nanjing First Hospital, Affiliated to Nanjing Medical University, 210006, Nanjing, Jiangsu, China

Abstract

The protracted nature of development makes the cerebellum vulnerable to a broad spectrum of pathologic conditions, especially during the early fetal period. This study aims to characterize normal cerebellar growth in human fetuses during the early second trimester. We manually segmented the fetal cerebellum using 7.0-T high-resolution MR images obtained in 35 specimens with gestational ages ranging from 15 to 22 weeks. Volume measurements and shape analysis were performed to quantitatively evaluate global and regional cerebellar growth. The absolute volume of the fetal cerebellum showed a quadratic growth with increasing gestational age, while the pattern of relative volume changes revealed that the cerebellum grew at a greater pace than the cerebrum after 17 gestational weeks. Shape analysis was used to examine the distinctive development of subregions of the cerebellum. The extreme lateral portions of both cerebellar hemispheres showed the lowest rate of growth. The anterior lobe grew faster than most of the posterior lobe. These findings expand our understanding of the early growth pattern of the human cerebellum and could be further used to assess the developmental conditions of the fetal brain.

*Corresponding author. liusw@sdu.edu.cn (S. Liu).
[1]F. Xu and X. Ge contributed equally to this work.

1. Introduction

The cerebellum has been increasingly recognized for its prominent role in brain development in recent years (Wang et al., 2014; D'Mello and Stoodley, 2015; Limperopoulos et al., 2010). In addition to well-established functions such as posture, balance, and motor coordination, the cerebellum has also been implicated in higher cognitive processes including executive control, language, and social emotion (Schmahmann and Sherman, 1997; Koziol et al., 2012; O'Halloran et al., 2012). Cerebellar dysfunction is associated with wide-ranging and long-term motor deficits, including Dandy-Walker symptom and Arnold-Chiari malformation (ten Donkelaar et al., 2003; Altman et al., 1992), as well as affective disorders, such as autism and schizophrenia (Allen et al., 2004; Hoppenbrouwers et al., 2008).

The development of the cerebellum spans a long period beginning in approximately the fourth week of gestation and lasting through the first postnatal year and follows a highly orchestrated process (ten Donkelaar et al., 2003). The basic morphology of the cerebellum, which results from neuronal proliferation, directional migration, and differentiation, is established around the 20th week of gestation (Rakic and Sidman, 1970; Leto et al., 2016). In the subsequent period up to 40 weeks of gestation, the cerebellum undergoes more rapid increases in volume and surface foliation than other cerebral structures (Limperopoulos et al., 2005; Clouchoux et al., 2012). Neuronal differentiation and white matter myelination of the cerebellum continue after birth (Yakovlev and Lecours, 1967). Its high complexity and protracted development makes the cerebellum particularly vulnerable to a wide range of developmental disorders, especially during the prenatal period (Poretti et al., 2016; Iruretagoyena et al., 2010).

However, little is known about cerebellar development during the early fetal developmental period because MR scans are not usually performed until the 19th gestational week (GW) in a clinical setting (Bendersky et al., 2008). The detailed anatomic delineation of the developing cerebellum is complicated to characterize, even when using 3.0-T MR *in vivo*, due to limited resolution, the small size of the cerebellum, frequent fetal movement, and the pulse of the maternal artery. The developmental differences between cerebellar subregions, which have distinct characteristics with regard to their embryological sources, phylogenetic histories, anatomical connections with the cerebral cortex, and functions (Ramnani, 2006), are thus difficult to distinguish. Postmortem fetal MR, on the other hand, offers advantages as an imaging modality by using high-field strength magnets, increasing acquisition times, and reducing slice thickness, thus providing value in studies of the developing fetal brain (Rados et al., 2006; Whitby et al., 2006; Kinoshita et al., 2001).

Quantitative measurements of the cerebellum, including its volume, the transverse cerebellar diameter, and the height and anterior-posterior diameter of the vermis, have been obtained in fetal, neonatal, and childhood populations (Hata et al., 2007; Zwicker et al., 2016; Tiemeier

et al., 2010). Quadratic growth was reported for both linear dimensions and the cerebellar volume in healthy fetuses (Triulzi et al., 2005; Hatab et al., 2008; Liu et al., 2011). The cerebellum also undergoes a dramatic change in its surface during the fetal period. Shape analysis provides enhanced sensitivity in reflecting local structural changes during development and has been widely used in the biomedical field to study various structures of interest, such as the hippocampus, thalamus, and corpus callosum (Thompson et al., 2004; Coscia et al., 2009; Joshi et al., 2013). Cerebellar regional differences in surface curvature were found in healthy fetuses aged 20–31 weeks of gestation (Scott et al., 2012). In particular, the apex of the vermis and the inferior-posterior lobe of the hemispheres increased in convexity, whereas the inferior surface of the vermis and the anterior lobe facing the brainstem increased in concavity. However, very few studies have applied shape analysis to evaluate the developing human cerebellum before 20 weeks of gestation.

The objective of this study was to quantify the development of the human cerebellum using 7.0-T high-resolution MR images obtained in 35 fetal specimens between 15 and 22 GW. The absolute and relative volumes of the cerebellum were both calculated to describe its developmental trajectory. Shape analysis was performed using our novel curvature-driven surface mapping algorithm, the Riemannian metric optimization on surfaces (RMOS) method (Gahm et al., 2018), to characterize the regional growth patterns of the fetal cerebellum. These results may be helpful for understanding the development of the cerebellum during the early second trimester and provide an anatomical reference for future cerebellar studies.

2. Materials and methods

2.1. Fetal specimens

Thirty-five normal human fetal specimens at 15–22 GW, which were partially or totally used to study fetal cerebral cortex, subcortical brain structures, the fetal brain template and the hippocampal formation in our previous publications (Zhang et al., 2013; Meng et al., 2012; Zhan et al., 2013; Ge et al., 2015), constituted the database for this study. They were collected in hospitals in Shandong Province, China. Some specimens were acquired following medically indicated abortions caused by teratogenesis infection, stressful intrauterine conditions, or unknown reasons related to malformation outside of the brain. The others were collected from spontaneous abortions attributed to maternal systemic infection, pregnancy-induced hypertension syndrome, severe uterine trauma caused by an accident, or uterine myoma. All specimens were first examined using ultrasound and 3.0-T MR prescans to ensure that the fetal brain was anatomically normal based on the size of the cerebrum and the developmental status of sulci, the lateral ventricle, and the corpus callosum. Maternal pregnancy records indicated no documented history of fetal chromosomal abnormality, maternal genetic disease, excessive alcohol intake, smoking, severe undernutrition, or eclampsia seizures.

Demographic information for the fetal specimens is provided in Table 1. The GW of the fetuses was estimated based on crown-rump length, head circumference, foot length, and/or pregnancy records and was expressed in weeks from the last menstrual period (Guihard-Costa et al., 2002). The specimens were kept immersed in 10% formalin for preservation

without extracting the brain. The time interval between the collection of specimens and scanning was less than two months. The formalin fixation time (in days) reported for each specimen is listed in Table 1. The time-length of formalin fixation had little impact on signal intensities in T2 images after 3–4 weeks (Tovi and Ericsson, 1992; Boyko et al., 1994), which was the minimum fixation time in our study to ensure tissue stability and comparability among subjects. This study was approved and controlled by the Internal Review Board of the Ethical Committee at the School of Medicine, Shandong University. Consent for postmortem examination was obtained from each parent.

2.2. MRI data acquisition

The specimens were scanned by a 7.0-T Micro-MR scanner with a maximum gradient of 360 mT (70/16 pharmaScan, Bruker Biospin GmbH, Germany) using a rat body coil with an inner diameter of 60 mm. 2D T2-weighted slice images were acquired in the axial plane with the following parameters: slice thickness, 0.5 mm (with no gap); TR/TE, 12,000/50 ms; field of view (FOV), 4.0×4.0 cm/5.0×5.0 cm/6.0×6.0 cm; matrix, 256×256; and NEX, 4. The acquisition time was 28 m 15 s.

2.3. Segmentation of the cerebellum

Based on prior studies (Hatab et al., 2008; Liu et al., 2011; Scott et al., 2012) and the 'Atlas of Human Central Nervous System Development' (Bayer and Altman, 2005), the anatomic boundaries of the cerebellum were manually delineated using ITK-SNAP software, a semiautomatic open source application with active contour evolution (Yushkevich et al., 2006). The segmentation was performed in the axial plane and confirmed in the sagittal and coronal planes. In the axial plane, the lateral hemispheres were clearly distinguished by the presence of cerebrospinal fluid (CSF) (Fig. 1A). The pontocerebellar angle was used to separate the cerebellar hemispheres from the pons. The major fissures of the cerebellum were easily observed on the sagittal plane (Fig. 1B). The first fissure to appear was the posterolateral fissure as early as 12–13 GW (Rakic and Sidman, 1970). The primary fissure, which divided the cerebellar anterior and posterior lobes, could be detected at 15 GW and was deepest in the midline (Fig. 1B). The cerebellar peduncles, brainstem, and the roof of the fourth ventricle were the main landmarks that defined the cerebellar anterior boundary. In the coronal plane, the caudal-most aspect of the hypothalamus was used to demarcate the superior border of the cerebellum (Fig. 1C).

To check the reproducibility of the manual segmentation protocol, ten specimens were chosen at random and resegmented by the same person at least one month later. The results of segmentation were checked and confirmed by two experienced anatomists. The intraclass correlation coefficient was measured with the strength of the agreement scale (Brennan and Silman, 1992).

2.4. Volume analysis

The segmentation of supratentorial brain was first accomplished using the methods described in our previous publication (Zhan et al., 2013). The supratentorial volumes (STV) included the entire cerebrum (telencephalon and diencephalon) but excluded the brainstem and cerebellum.

The absolute cerebellar volume and STV were calculated. The relative volume of the cerebellum was defined as the ratio of cerebellar absolute volume to the sum of the cerebellar and supratentorial volumes ($V_{relative} = V_{absolute}/(V_{absolute} + STV)$).

2.5. Template construction

To improve the accuracy of the registration step of the shape analysis, a template of the fetal cerebellum was first constructed using the optimal template construction function of Advanced Normalization Tools (ANTs) (Avants et al., 2009). The script *buildtemplateparallel. sh* (Avants and Gee, 2004) was run for all specimens using the default setting in ANTs. Specifically, we used symmetric diffeomorphic normalization (SyN) energy terms, which performed image normalization by minimizing image similarity and the diffeomorphism length of the diffeomorphic transformations (Avants et al., 2008). The ANTs-SyN approach was defined by the minimum shape and appearance distance on the image. It maintained symmetry when using pairwise mapping. The process was iteratively repeated, and the final template was constructed at the minimum energy level.

2.6. Shape analysis

A previously validated shape analysis approach (Ge et al., 2015) was used to measure cerebellar local changes. To perform surface mapping, the binary masks of each subject and the template were first converted to triangular meshes. The spurious features caused by segmentation artifacts were detected and removed using iterated Laplace–Beltrami (LB) eigen-projection and boundary deformation (Shi et al., 2010). The resulting surface meshes, which represented the correct topology of the cerebellum, were remeshed to obtain 3000 uniformly distributed vertices (Fig. 2B). The number of vertices (3000) was determined according to the size of the cerebellum during the early second trimester.

Each individual triangulated mesh was then registered to our constructed cerebellar template mesh using the novel curvature-driven surface mapping algorithm, Riemannian metric optimization on surfaces (RMOS), which incorporated both geometric and anatomical features to guide surface mapping in the LB embedding space (Gahm et al., 2018). For the cerebellum, the mean curvature feature was used to drive the surface mapping process. For each triangular mesh, the Riemannian metric was denoted as a set of weights defined on all edges and fully determined the heat kernel on the mesh (Zeng et al., 2012; Goes et al., 2014). The RMOS approach can be used to iteratively optimize the Riemannian metric to match the curvature feature and realize surface mapping in the LB embedding space (Gahm et al., 2018). As a result, all surfaces were represented with the same triangulation, and the vertices were in one-to-one correspondence. To quantify the local rate of growth of the cerebellum, similar to methods used for shape analysis of the hippocampus (Shi et al., 2009), the thickness measured at each vertex of the mapped surfaces was defined as the distance from the vertex to the medial core of the cerebellum.

2.7. Statistical analysis

Polynomial regression analysis was performed to determine the best-fit model using gestational weeks as the independent variable and absolute cerebellum volumes as the dependent variable. The R^2 value was calculated. To model the local development of the

fetal cerebellum, the thicknesses associated with increasing gestational age were measured by linear regression analysis. The p-value and regression coefficient were calculated. Correction for multiple comparisons was performed using a false discovery rate (FDR) at q value of 0.05.

3. Results

3.1. Segmentation reliability

The average intraclass correlation coefficient was 0.9639, indicating our segmentation method showed good reproducibility.

3.2. Volume analysis

As shown in Fig. 3A, the absolute volume of the cerebellum increased approximately 5.3-fold from 0.3 to 1.6 cm^3 across the selected GW range. The growth rate steadily increased, and the second polynomial model ($R^2 = 0.9475$) better fit the growth trajectory than a linear model ($R^2 = 0.9181$).

The relative volume curve of the cerebellum remained nearly horizontal from 15 to 17 GW and began to gradually increased after 17 GW (Fig. 3B). This curve suggested that the cerebellum had a growth rate similar to that of the supratentorial brain before 17 GW and outstripped it after 17 GW.

3.3. Shape analysis

The results of the shape analysis were mapped onto the template surface of the cerebellum, as shown in Fig. 4. The cerebellar template was dumbbell-shaped with two lateral hemispheres and a relatively thin vermis. The regression coefficients represented the growth rate of the local cerebellum, and p-values were calculated from linear regression of the corresponding thickness of 3000 vertices.

From 15 to 22 GW, thickness increased significantly throughout nearly the whole cerebellum, except for the extreme lateral portions of both hemispheres (Fig. 4A). The central part of the anterior cerebellar surface adjacent to the brainstem grew more slowly than its surroundings. For the posterior surface of the cerebellum, the degree of increase for the two hemispheres was high. The apex of the vermis increased at a faster rate than the adjacent parts of the hemispheres in the cerebellar superior surface, whereas the inferior–posterior surface of the vermis grew comparatively slowly. Overall, the cerebellar anterior lobe had a faster rate of growth than most of the posterior lobe, and the subregions of the posterior lobe increased in a nonhomogeneous manner (Fig. 4B).

4. Discussion

We calculated the absolute and relative volumes of the fetal cerebellum and investigated its regional growth patterns during the early second trimester. The absolute volume of the fetal cerebellum followed a quadratic growth trajectory, while the relative volume tendency suggested faster growth than the cerebrum after 17 GW. Shape analysis demonstrated that both extreme lateral portions of the cerebellar hemispheres had a significantly lower rate of

growth compared with the other regions, and the anterior lobe grew faster than most of the posterior lobe during the period from 15 to 22 GW.

4.1. Volume analysis

In the current study, the growth trajectory of the cerebellar absolute volume during the early second trimester was best fitted by the second-order polynomial regression curve (Fig. 3A). The result was in good agreement with previous ultrasound and MRI studies of fetuses ranging in age from 16 to 40 GW (Chang et al., 2000; Hatab et al., 2008; Vatansever et al., 2013). The quadratic growth pattern indicated that the pattern of cerebellar volume growth accelerated over the prenatal period. However, some studies have conducted linear regression analyses of cerebellar volume growth in fetuses and preterm infants (Limperopoulos et al., 2005; Clouchoux et al., 2012). The differences in volume calculations among these studies may have resulted from the use of different anisotropic resolutions, segmentation protocols, and gestational age estimation methods. We reported that the absolute volume of the fetal cerebellum showed a 5.3-fold increase (from 0.3 to 1.6 cm^3) during the gestational period between 15 and 22 weeks. A 14-fold increase (from 1.6 to 22.9 cm^3) in cerebellar volume was observed from 21.71 to 38.89 GW based on *in vivo* MRI (Vatansever et al., 2013). Therefore, the cerebellum maintains a rapid rate of growth in volume during the second and third trimesters.

We found that the growth rate of the cerebellum exceeded that of the cerebrum after 17 GW (Fig. 3B). As assessed by 3-D MRI and ultrasound, the cerebellum increased in volume more rapidly than the cerebrum did from 20 to 44 GW (Limperopoulos et al., 2005; Scott et al., 2012; Kyriakopoulou et al., 2017). According to weight measurements, the proportion of the cerebellum to the total brain steadily increased after 19 GW (Guihard-Costa and Larroche, 1990). During the development of the cerebral cortex, neurons were generated in the ventricular and subventricular zones and migrated outwards to the pial surface, whereas cerebellar growth was marked by the inward migration of cells from the external to the internal granular layers (Sidman and Rakic, 1973). Beginning around the 16th GW, the postmitotic granule cells from the external granular layer migrated inwards, and the Purkinje cells enlarged in size and developed apical dendritic trees (ten Donkelaar et al., 2003; Sidman and Rakic, 1973). These cellular developments may be related to the faster growth of the cerebellum. In addition, the relative volume of the cerebellum showed a more prominent increase during the postnatal period. The total brain volume increased by 101% in the first year, whereas the cerebellar volume showed a significantly greater increase of 240% (Knickmeyer et al., 2008). Taken together, the greater growth pattern of the cerebellum compared to the cerebrum may begin as early as the 17th GW and continue until the early postnatal period.

4.2. Shape analysis

We constructed a template representing the average surface of the cerebellum at early gestational ages (from 15 to 22 GW), during which it showed a dumbbell shape (Fig. 2) that was different from the inverted heart shape observed from 20 to 31 GW (Scott et al., 2012). During the second and third trimesters, the cerebellum exhibited rapid growth, including an increase in surface foliation, deepening of the primary fissures, and the emergence of

secondary fissures (Chong et al., 1997; Lavezzi et al., 2006). These developments may underlie the remarkable changes that occur in the shape of the cerebellum.

Studies on cellular development found that the cerebellar cortex underwent greater cell proliferation along the longitudinal axis during the third and fifth months of pregnancy (Keibel and Mall, 1912; Patten, 1968). Specifically, longitudinal growth occurred earlier in the vermis and later extended to the cerebellar hemispheres (Keibel and Mall, 1912). In a study of measurements of cerebellar linear dimensions, the height and anterior-posterior diameter of the vermis were found to increase by 220% and 208%, respectively, and these increases were greater than that found along the transverse cerebellar diameter (180%) between 19 and 37 weeks of gestation (Triulzi et al., 2005). Our results, based on the shape analysis method, showed that the extreme lateral portions of the cerebellar hemispheres had the slowest growth during the early second trimester (Fig. 4A). Overall, the cerebellar hemispheres developed later than the vermis in the early fetal period. According to phylogenetic criteria, the vermis belongs to the paleocerebellum, and the cerebellar hemispheres belong to the neocerebellum. The phylogenetically older parts of the cerebellum develop earlier than the younger parts, in accordance with cerebral cortical development (Gogtay et al., 2004). The cerebellum was characterized by transverse growth during the third trimester (Malinger et al., 2001; Tubbs and Oakes, 2013). Adolescents born severely prematurely showed significantly reduced cerebellar volume, especially in the lateral lobes (Allin et al., 2005). A study of preterm newborns showed that the rate of volume expansion was higher in the lateral convexity of the cerebellar hemispheres (Kim et al., 2016). The hemispheres of the cerebellum, especially the lateral portions, may undergo more rapid growth in the late fetal period.

The differences in the regional development features of the cerebellum observed in this study may be associated with functional topography. The cerebellum is divided into two large main lobes (the anterior lobe and the posterior lob) by the primary fissures. Our results showed that the anterior lobe of the cerebellum grew faster than most of the posterior lobe between 15 and 22 GW (Fig. 4B). Prior cerebellar functional connectivity and task-related studies have shown that the anterior lobe was mainly involved in sensorimotor control, while the majority of the posterior lobe, which was interconnected with cerebral association cortices, participated in cognitive and emotional processing (Buckner et al., 2011; O'Reilly et al., 2010; Stoodley and Schmahmann, 2009; Stoodley et al., 2012). The cerebral association cortices participate in a range of cognitive processes and mature later in development (Fuster, 2002; Gogtay et al., 2004). Thus, we cautiously propose that the different growth rates of the cerebellar subregions are related to their functional characteristics. In addition, the regions of the cerebral cortex and the cerebellum that participate in cognitive processing mature later than other regions. There may be similar trajectories of growth within cerebro-cerebellar circuits.

The growth of the superior surface of the cerebellum was faster than that of its inferior regions (Fig. 4B). This may be due to evolution, in that the superior regions of the cerebellum received granular cells earlier than the inferior regions (Altman and Bayer, 1978). The inferior-posterior part of the vermis grew more slowly than its surrounding structures (Fig. 4B, inferior view), which may be associated with the increase in the

curvature of the posterolateral fissure that occurred from 15 to 28 GW (Nowakowska-Kotas et al., 2014). Additionally, changes in surface shape statistics may reflect the influence of the surrounding tissues. The relatively slower growth along the central part of the anterior cerebellar surface (Fig. 4B, anterior view) appeared to be caused by the expansion of the brainstem. The posterior surface of the two hemispheres exhibited rapid growth (Fig. 4B, posterior view), which may have been promoted by the surrounding vacant space. These results were consistent with previous observations of the cerebellar surface curvature (Scott et al., 2012). From 21 to 30 GW, the anterior lobe facing the brainstem of the hemispheres increased in concavity, while the inferior-posterior lobe of the cerebellar hemispheres increased in convexity.

In summary, cerebellar subdivisions based on phylogenetic and functional characteristics showed distinct patterns of growth in this study that may be related to their roles in different aspects of development.

4.3. Limitations and future directions

This study has several limitations. We did not measure hemispheric differences in cerebellar volume. While structural and functional asymmetries have been identified in the adult cerebellum (Wang et al., 2013), Scott found that there was no significant difference between the right and left hemispheric volumes of fetal cerebellum from 20 to 31 GW (Scott et al., 2012). Our sample size was too small to perform analysis of sex-based differences in fetal cerebellar development. Sex differences in cerebellar volume have been observed in childhood and adolescence (Brain Development Cooperative, 2012; Wierenga et al., 2014). However, virtually no studies have evaluated sex differences in cerebellar growth in fetuses or children younger than 3 years old.

In this study, we included fetal specimens obtained during medically indicated abortions that were attributed to stressful intrauterine conditions or teratogenesis infection. However, we set strict specimen inclusion criteria, and 35 specimens were chosen from a total of 49 fetuses at 15–22 GW. Ultrasound and 3.0-T MR prescans were conducted by two pediatric neuro-radiologists to ensure that the fetal brain was anatomically normal based on the size of the cerebrum and the developmental status of sulci, the lateral ventricle, and the corpus callosum. Fetuses for which there was a discrepancy between the two radiologists about brain development were excluded, and only fetuses with a morphologically normal central nervous system were included in this study. In addition, the maternal pregnancy records indicated no documented history of fetal chromosomal abnormality, maternal genetic disease, excessive alcohol intake, smoking, severe undernutrition, or eclampsia seizures.

Another limitation of our study is that the morphological differences between formalin-fixed samples and *in vivo* brains should be considered when applying the present results to clinical observations. Tissue degradation caused by formalin fixation is common in postmortem studies (Stan et al., 2006), and minor tissue degradation may slightly affect volume measurements and shape statistical results. However, the MRI scans performed in this study were acquired while the brain was in the skull, and the time interval between the collection of specimens and the MRI scans was less than two months in order to minimize tissue degradation. Although the results presented in this study cannot be directly used in clinical

diagnoses, they provide information that is beneficial for evaluating fetal cerebellar development and can be used as a reference for MRI examinations obtained at lower field strengths (Lin et al., 2011).

Moreover, another limitation of our study is that we made no histological sections to compare results to those obtained via high-resolution MR images because fetal specimens are extremely difficult to obtain. Due to the limitation of materials, this study was performed using cross-sectional rather than longitudinal analysis to characterize global and regional growth of the cerebellum during the early second trimester.

Early anatomical and embryological studies have established MRI templates of the cerebellum based on formalin-fixed normal fetal specimens at gestational ages ranging between 9 and 28 weeks (Chong et al., 1997; Nakayama and Yamada, 1999). However, those templates described only normal cerebellar development features and could not be used to improve automated segmentation of fetal cerebellar studies. A spatiotemporal atlas including the cerebellum has been constructed for the premature and postnatal brain from 28 to 47 GW (Kuklisova--Murgasova et al., 2011). In future studies, we will continue to collect more fetal data and construct a spatiotemporal atlas of the cerebellum at each gestational week, and this will significantly improve the automatic analysis of cerebellum MRI data.

5. Conclusions

In this study, we characterized 3D morphological development of fetal cerebellum during the early second trimester using 7.0-T high-resolution MR images. The advanced shape analysis method revealed that different cerebellar subregions exhibited distinctive developmental trajectories. The absolute and relative volumes of the cerebellum were both determined. Our results complement our current knowledge of the early growth pattern of the human cerebellum and may prove valuable in improving understanding of cerebellar dysmorphology, both neurological and psychological.

Acknowledgments

References

Allen G, Muller RA, Courchesne E, 2004 Cerebellar function in autism: functional magnetic resonance image activation during a simple motor task. Biol. Psychiatry 56, 269–278. [PubMed: 15312815]

Allin MPG, Salaria S, Nosarti C, Wyatt J, Rifkin L, Murray RM, 2005 Vermis and lateral lobes of the cerebellum in adolescents born very preterm. Neuroreport 16, 1821–1824. [PubMed: 16237334]

Altman J, Bayer SA, 1978 Prenatal development of the cerebellar system in the rat. I. Cytogenesis and histogenesis of the deep nuclei and the cortex of the cerebellum.J. Comp. Neurol 179, 23–48. [PubMed: 8980716]

Altman NR, Naidich TP, Braffman BH, 1992 Posterior-Fossa malformations. Am. J.Neuroradiol 13, 691–724. [PubMed: 1566724]

Avants B, Gee JC, 2004 Geodesic estimation for large deformation anatomical shape averaging and interpolation. Neuroimage 23 (Suppl. 1), S139–S150. [PubMed: 15501083]

Avants BB, Epstein CL, Grossman M, Gee JC, 2008 Symmetric diffeomorphic image registration with cross-correlation: evaluating automated labeling of elderly and neurodegenerative brain. Med. Image Anal 12, 26–41. [PubMed: 17659998]

Avants BB, Tustison N, Song G, 2009 Advanced normalization tools (ANTS). Insight j 2, 1–35.

Bayer SA, Altman J, 2005 The Human Brain during the Second Trimester (Atlas of the Human Central Nervous System Development). CRC Press, Indianapolis.

Bendersky M, Tamer I, Van Der Velde J, Dunaievsky A, Schuster G, Rugilo C, Sica RE, 2008 Prenatal cerebral magnetic resonance imaging. J. Neurol. Sci 275, 37–41. [PubMed: 18760424]

Boyko O, Alston S, Fuller G, Hulette C, Johnson G, Burger P, 1994 Utility of postmortem magnetic resonance imaging in clinical neuropathology. Arch. Pathol. Lab Med 118, 219–225. [PubMed: 8135623]

Brain Development Cooperative, G., 2012 Total and regional brain volumes in a population-based normative sample from 4 to 18 years: the NIH MRI Study of Normal Brain Development. Cerebr. Cortex 22, 1–12.

Brennan P, Silman A, 1992 Statistical methods for assessing observer variability in clinical measures. BMJ Br. Med. J. (Clin. Res. Ed.) 304, 1491.

Buckner RL, Krienen FM, Castellanos A, Diaz JC, Yeo BT, 2011 The organization of the human cerebellum estimated by intrinsic functional connectivity.J. Neurophysiol 106, 2322–2345. [PubMed: 21795627]

Chang CH, Chang FM, Yu CH, Ko HC, Chen HY, 2000 Assessment of fetal cerebellar volume using three-dimensional ultrasound. Ultrasound Med. Biol 26, 981–988. [PubMed: 10996698]

Chong BW, Babcook CJ, Pang D, Ellis WG, 1997 A magnetic resonance template for normal cerebellar development in the human fetus. Neurosurgery 41, 924–929. [PubMed: 9316055]

Clouchoux C, Guizard N, Evans AC, du Plessis AJ, Limperopoulos C, 2012 Normative fetal brain growth by quantitative in vivo magnetic resonance imaging. Am. J. Obstet. Gynecol 206, 173 e171–178. [PubMed: 22055336]

Coscia DM, Narr KL, Robinson DG, Hamilton LS, Sevy S, Burdick KE, Gunduz-Bruce H, McCormack J, Bilder RM, Szeszko PR, 2009 Volumetric and shape analysis of the thalamus in first-episode schizophrenia. Hum. Brain Mapp 30, 1236–1245. [PubMed: 18570200]

D 'Mello AM, Stoodley CJ, 2015 Cerebro-cerebellar circuits in autism spectrum disorder. Front. Neurosci 9, 408. [PubMed: 26594140]

Fuster JM, 2002 Frontal lobe and cognitive development. J. Neurocytol 31, 373–385. [PubMed: 12815254]

Gahm JK, Shi Y, Alzheimer's Disease Neuroimaging I, 2018 Riemannian metric optimization on surfaces (RMOS) for intrinsic brain mapping in the Laplace-Beltrami embedding space. Med. Image Anal 46, 189–201. [PubMed: 29574399]

Ge X, Shi Y, Li J, Zhang Z, Lin X, Zhan J, Ge H, Xu J, Yu Q, Leng Y, Teng G, Feng L, Meng H, Tang Y, Zang F, Toga AW, Liu S, 2015 Development of the human fetal hippocampal formation during early second trimester. Neuroimage 119, 33–43. [PubMed: 26123377]

Goes F.d., Memari P, Mullen P, Desbrun M, 2014 Weighted triangulations for geometry processing. ACM Trans. Graph 33, 1–13.

Gogtay N, Giedd JN, Lusk L, Hayashi KM, Greenstein D, Vaituzis AC,Nugent TF, Herman DH, Clasen LS, Toga AW, 2004 Dynamic mapping of human cortical development during childhood through early adulthood. P Natl Acad Sci USA 101, 8174–8179.

Guihard-Costa A-M, Larroche J-C, 1990 Differential growth between the fetal brain and its infratentorial part. Early Hum. Dev 23, 27–40. [PubMed: 2209474]

Guihard-Costa AM, Menez F, Delezoide AL, 2002 Organ weights in human fetuses after formalin fixation: standards by gestational age and body weight. Pediatr. Dev. Pathol 5, 559–578. [PubMed: 12399830]

Hata T, Kuno A, Dai SY, Inubashiri E, Hanaoka U, Kanenishi K, Yamashiro C,Tanaka H, Yanagihara T, 2007 Three-dimensional sonographic volume measurement of the fetal cerebellum. J. Med. Ultrason 34 (2001), 17–21.

Hatab MR, Kamourieh SW, Twickler DM, 2008 MR volume of the fetal cerebellum in relation to growth. J. Magn. Reson. Imaging 27, 840–845. [PubMed: 18302203]

Hoppenbrouwers SS, Schutter DJ, Fitzgerald PB, Chen R, Daskalakis ZJ, 2008 The role of the cerebellum in the pathophysiology and treatment of neuropsychiatric disorders: a review. Brain Res. Rev 59, 185–200. [PubMed: 18687358]

Iruretagoyena JI, Trampe B, Shah D, 2010 Prenatal diagnosis of Chiari malformation with syringomyelia in the second trimester. J. Matern. Fetal Neonatal Med 23, 184–186. [PubMed: 19572237]

Joshi SH, Narr KL, Philips OR, Nuechterlein KH, Asarnow RF, Toga AW, Woods RP, 2013 Statistical shape analysis of the corpus callosum in Schizophrenia. Neuroimage 64, 547–559. [PubMed: 23000788]

Keibel F, Mall FP, 1912 Manual of Human Embryology, vol. 2 JB Lippincott Company, pp. 67–74.

Kim H, Gano D, Ho ML, Guo XM, Unzueta A, Hess C, Ferriero DM, Xu D, Barkovich AJ, 2016 Hindbrain regional growth in preterm newborns and its impairment in relation to brain injury. Hum. Brain Mapp 37, 678–688. [PubMed: 26589992]

Kinoshita Y, Okudera T, Tsuru E, Yokota A, 2001 Volumetric analysis of the germinal matrix and lateral ventricles performed using MR images of postmortem fetuses. Am. J. Neuroradiol 22, 382–388. [PubMed: 11156787]

Knickmeyer RC, Gouttard S, Kang C, Evans D, Wilber K, Smith JK, Hamer RM, Lin W, Gerig G, Gilmore JH, 2008 A structural MRI study of human brain development from birth to 2 years. J. Neurosci 28, 12176–12182. [PubMed: 19020011]

Koziol LF, Budding DE, Chidekel D, 2012 From movement to thought: executive function, embodied cognition, and the cerebellum. Cerebellum 11, 505–525. [PubMed: 22068584]

Kuklisova-Murgasova M, Aljabar P, Srinivasan L, Counsell SJ, Doria V, Serag A, Gousias IS, Boardman JP, Rutherford MA, Edwards AD, Hajnal JV, Rueckert D, 2011 A dynamic 4D probabilistic atlas of the developing brain. Neuroimage 54, 2750–2763. [PubMed: 20969966]

Kyriakopoulou V, Vatansever D, Davidson A, Patkee P, Elkommos S, Chew A, Martinez-Biarge M, Hagberg B, Damodaram M, Allsop J, Fox M, Hajnal JV, Rutherford MA, 2017 Normative biometry of the fetal brain using magnetic resonance imaging. Brain Struct. Funct 222, 2295–2307. [PubMed: 27885428]

Lavezzi AM, Ottaviani G, Terni L, Matturri L, 2006 Histological and biological developmental characterization of the human cerebellar cortex. Int. J. Dev. Neurosci 24, 365–371. [PubMed: 16893622]

Leto K, Arancillo M, Becker EB, Buffo A, Chiang C, Ding B, Dobyns WB, Dusart I, Haldipur P, Hatten ME, Hoshino M, Joyner AL, Kano M, Kilpatrick DL, Koibuchi N, Marino S, Martinez S, Millen KJ, Millner TO, Miyata T, Parmigiani E, Schilling K, Sekerkova G, Sillitoe RV, Sotelo C, Uesaka N, Wefers A, Wingate RJ, Hawkes R, 2016 Consensus paper: cerebellar development. Cerebellum 15, 789–828. [PubMed: 26439486]

Limperopoulos C, Chilingaryan G, Guizard N, Robertson RL, Du Plessis AJ, 2010 Cerebellar injury in the premature infant is associated with impaired growth of specific cerebral regions. Pediatr. Res 68, 145. [PubMed: 20389260]

Limperopoulos C, Soul JS, Gauvreau K, Huppi PS, Warfield SK, Bassan H, Robertson RL, Volpe JJ, du Plessis AJ, 2005 Late gestation cerebellar growth is rapid and impeded by premature birth. Pediatrics 115, 688–695. [PubMed: 15741373]

Lin X, Zhang Z, Teng G, Meng H, Yu T, Hou Z, Fang F, Zang F, Liu S, 2011 Measurements using 7.0 T post-mortem magnetic resonance imaging of the scalar dimensions of the fetal brain between 12 and 20 weeks gestational age. Int. J. Dev. Neurosci 29, 885–889. [PubMed: 21820045]

Liu F, Zhang Z, Lin X, Teng G, Meng H, Yu T, Fang F, Zang F, Li Z, Liu S, 2011 Development of the human fetal cerebellum in the second trimester: a post mortem magnetic resonance imaging evaluation. J. Anat 219, 582–588. [PubMed: 21812776]

Malinger G, Ginath S, Lerman-Sagie T, Watemberg N, Lev D, Glezerman M, 2001 The fetal cerebellar vermis: normal development as shown by transvaginal ultrasound. Prenat. Diagn 21, 687–692. [PubMed: 11536272]

Meng H, Zhang Z, Geng H, Lin X, Feng L, Teng G, Fang F, Zang F, Liu S, 2012 Development of the subcortical brain structures in the second trimester: assessment with 7.0-T MRI. Neuroradiology 54, 1153–1159. [PubMed: 22811291]

Nakayama T, Yamada R, 1999 MR imaging of the posterior fossa structures of human embryos and fetuses. Radiat. Med 17, 105–114. [PubMed: 10399777]

Nowakowska-Kotas M, Kedzia A, Dudek K, 2014 Development of external surfaces of human cerebellar lobes in the fetal period. Cerebellum 13, 541–548. [PubMed: 24831768]

O 'Halloran CJ, Kinsella GJ, Storey E, 2012 The cerebellum and neuropsychological functioning: a critical review. J. Clin. Exp. Neuropsychol 34, 35–56. [PubMed: 22047489]

O 'Reilly JX, Beckmann CF, Tomassini V, Ramnani N, Johansen-Berg H, 2010 Distinct and overlapping functional zones in the cerebellum defined by resting state functional connectivity. Cerebr. Cortex 20, 953–965.

Patten BM, 1968 Human Embryology, vol. 3 McGraw-Hill Book Company, Inc., New York, pp. 280–282.

Poretti A, Boltshauser E, Huisman TA, 2016 Prenatal cerebellar disruptions: neuroimaging spectrum of findings in correlation with likely mechanisms and etiologies of injury. Neuroimaging Clin. N. Am 26, 359–372. [PubMed: 27423799]

Rados M, Judas M, Kostovic I, 2006 In vitro MRI of brain development. Eur. J. Radiol 57, 187–198. [PubMed: 16439088]

Rakic P, Sidman RL, 1970 Histogenesis of cortical layers in human cerebellum, particularly the lamina dissecans. J. Comp. Neurol 139, 473–500. [PubMed: 4195699]

Ramnani N, 2006 The primate cortico-cerebellar system: anatomy and function. Nat.Rev. Neurosci. 7, 511–522.

Schmahmann JD, Sherman JC, 1997 Cerebellar cognitive affective syndrome. Int.Rev. Neurobiol. 41, 433–440.

Scott JA, Hamzelou KS, Rajagopalan V, Habas PA, Kim K, Barkovich AJ, Glenn OA, Studholme C, 2012 3D morphometric analysis of human fetal cerebellar development. Cerebellum 11, 761–770. [PubMed: 22198870]

Shi Y, Lai R, Morra JH, Dinov I, Thompson PM, Toga AW, 2010 Robust surface reconstruction via Laplace-Beltrami eigen-projection and boundary deformation. IEEE Trans. Med. Imaging 29, 2009–2022. [PubMed: 20624704]

Shi Y, Morra JH, Thompson PM, Toga AW, 2009 Inverse-consistent surface mapping with Laplace-Beltrami eigen-features In: International Conference on Information Processing in Medical Imaging. Springer, pp. 467–478.

Sidman RL, Rakic P, 1973 Neuronal migration, with special reference to developing human brain: a review. Brain Res. 62, 1–35. [PubMed: 4203033]

Stan AD, Ghose S, Gao XM, Roberts RC, Lewis-Amezcua K, Hatanpaa KJ, Tamminga CA, 2006 Human postmortem tissue: what quality markers matter? Brain Res. 1123, 1–11. [PubMed: 17045977]

Stoodley CJ, Schmahmann JD, 2009 Functional topography in the human cerebellum: a meta-analysis of neuroimaging studies. Neuroimage 44, 489–501. [PubMed: 18835452]

Stoodley CJ, Valera EM, Schmahmann JD, 2012 Functional topography of the cerebellum for motor and cognitive tasks: an fMRI study. Neuroimage 59, 1560–1570. [PubMed: 21907811]

ten Donkelaar HJ, Lammens M, Wesseling P, Thijssen HO, Renier WO, 2003 Development and developmental disorders of the human cerebellum. J. Neurol 250, 1025–1036. [PubMed: 14504962]

Thompson PM, Hayashi KM, De Zubicaray GI, Janke AL, Rose SE, Semple J, Hong MS, Herman DH, Gravano D, Doddrell DM, Toga AW, 2004 Mapping hippocampal and ventricular change in Alzheimer disease. Neuroimage 22, 1754–1766. [PubMed: 15275931]

Tiemeier H, Lenroot RK, Greenstein DK, Tran L, Pierson R, Giedd JN, 2010 Cerebellum development during childhood and adolescence: a longitudinal morphometric MRI study. Neuroimage 49, 63–70. [PubMed: 19683586]

Tovi M, Ericsson A, 1992 Measurements of T1 and T2 over time in formalin-fixed human whole-brain specimens. Acta Radiol. 33, 400–404. [PubMed: 1389643]

Triulzi F, Parazzini C, Righini A, 2005 MRI of fetal and neonatal cerebellar development. Semin. Fetal Neonatal Med 10, 411–420. [PubMed: 15985392]

Tubbs RS, Oakes WJ, 2013 The Chiari Malformations. Springer, pp. 35–41.

Vatansever D, Kyriakopoulou V, Allsop JM, Fox M, Chew A, Hajnal JV, Rutherford MA, 2013 Multidimensional analysis of fetal posterior fossa in health and disease. Cerebellum 12, 632–644. [PubMed: 23553467]

Wang D, Buckner RL, Liu H, 2013 Cerebellar asymmetry and its relation to cerebral asymmetry estimated by intrinsic functional connectivity. J. Neurophysiol 109, 46–57. [PubMed: 23076113]

Wang SS, Kloth AD, Badura A, 2014 The cerebellum, sensitive periods, and autism.Neuron 83, 518–532. [PubMed: 25102558]

Whitby EH, Paley MNJ, Cohen M, Griffiths PD, 2006 Post-mortem fetal MRI: what do we learn from it? Eur. J. Radiol 57, 250–255. [PubMed: 16413985]

Wierenga L, Langen M, Ambrosino S, van Dijk S, Oranje B, Durston S, 2014Typical development of basal ganglia, hippocampus, amygdala and cerebellum from age 7 to 24. Neuroimage 96, 67–72. [PubMed: 24705201]

Yakovlev PL, Lecours AR, 1967 The myelogenetic cycles of regional maturation of the brain. Reg. Develop. Brain Early Life 3–70.

Yushkevich PA, Piven J, Hazlett HC, Smith RG, Ho S, Gee JC, Gerig G, 2006 User-guided 3D active contour segmentation of anatomical structures: significantly improved efficiency and reliability. Neuroimage 31, 1116–1128. [PubMed: 16545965]

Zeng W, Guo R, Luo F, Gu X, 2012 Discrete heat kernel determines discrete Riemannian metric. Graph. Model 74, 121–129.

Zhan J, Dinov ID, Li J, Zhang Z, Hobel S, Shi Y, Lin X, Zamanyan A, Feng L, Teng G, Fang F, Tang Y, Zang F, Toga AW, Liu S, 2013 Spatial-temporal atlas of human fetal brain development during the early second trimester. Neuroimage 82, 115–126. [PubMed: 23727529]

Zhang Z, Hou Z, Lin X, Teng G, Meng H, Zang F, Fang F, Liu S, 2013Development of the fetal cerebral cortex in the second trimester: assessment with 7T postmortem MR imaging. AJNR Am J Neuroradiol 34, 1462–1467. [PubMed: 23413246]

Zwicker JG, Miller SP, Grunau RE, Chau V, Brant R, Studholme C, Liu M,Synnes A, Poskitt KJ, Stiver ML, Tam EW, 2016 Smaller cerebellar growth and poorer neurodevelopmental outcomes in very preterm infants exposed to neonatal morphine. J. Pediatr. Urol 172, 81–87 e82.
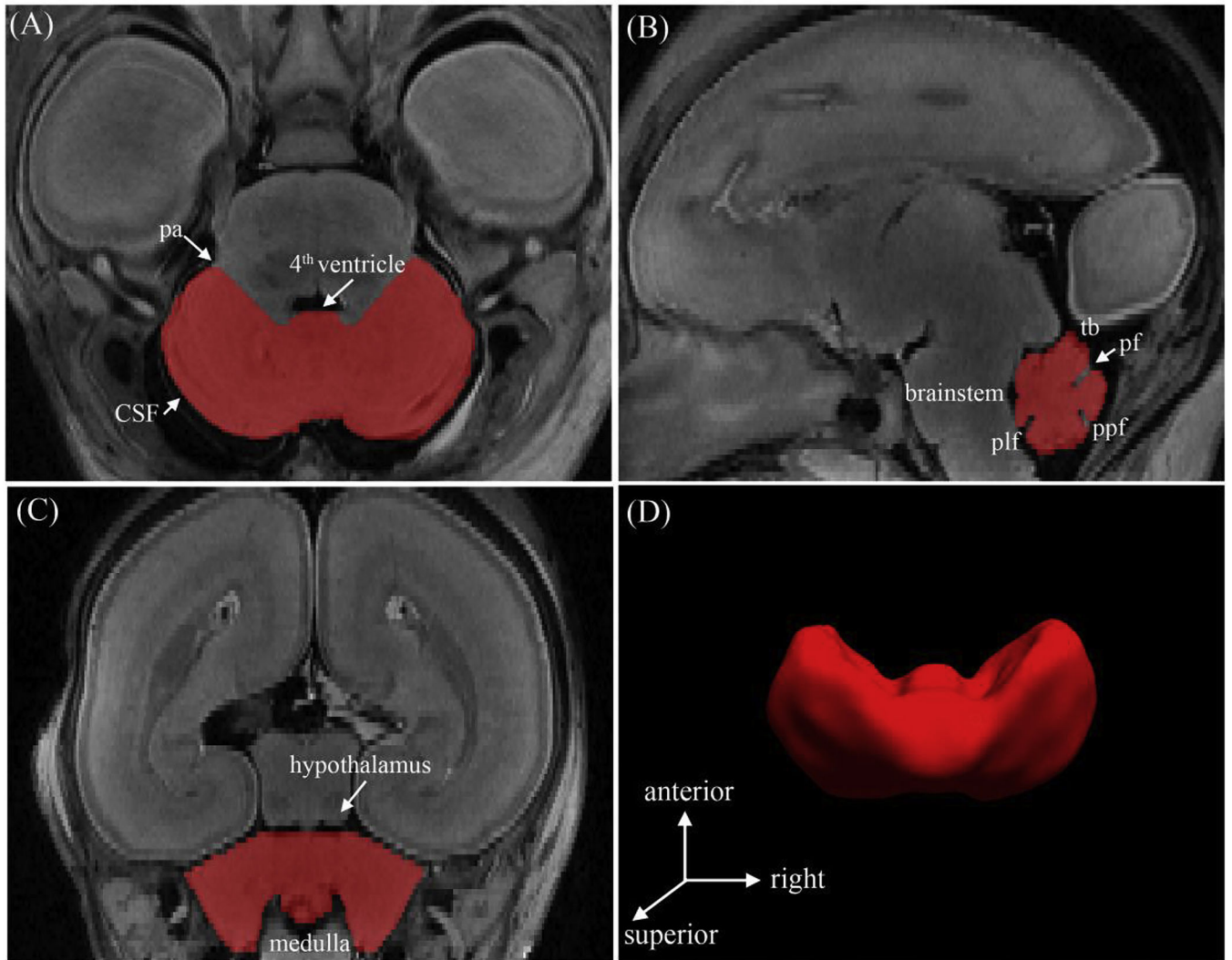
Fig. 1.
Segmentation and surface reconstruction of the cerebellum of a 20 GW subject. The boundaries of the cerebellum were delineated in the axial plane (a) and confirmed in the sagittal (b) and coronal (c) planes to verify the segmentation accuracy. (d) The 3D reconstructed cerebellar surface was displayed simultaneously. Abbreviations: (pa) pontocerebellar angle; (tb) tentorium cerebelli; (pf) primary fissure; (ppf) prepyramidal fissure; (plf) posterolateral fissure.

(A)

(B)

Anterior
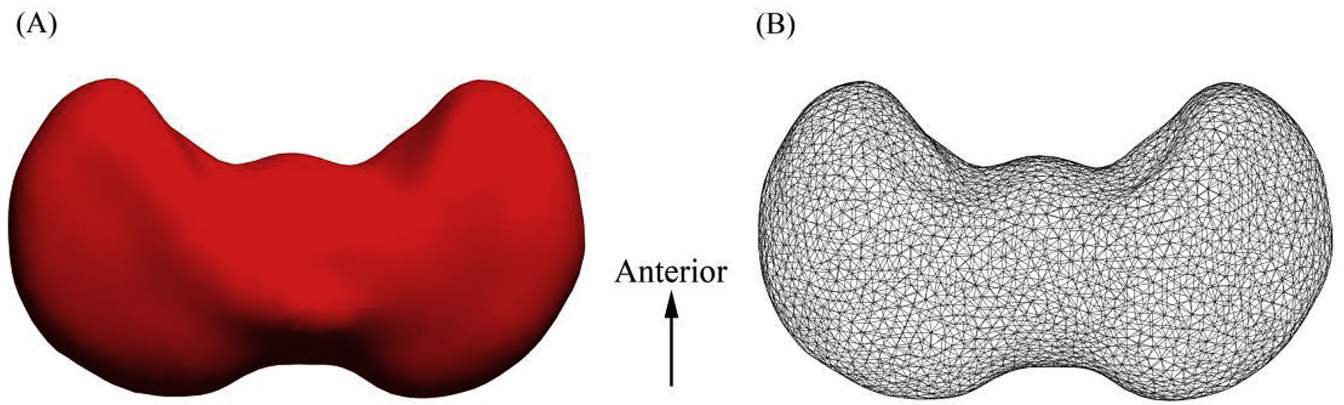
Fig. 2.
Superior view of the 3D representation model of the cerebellar template (A) and its corresponding surface meshes (B).
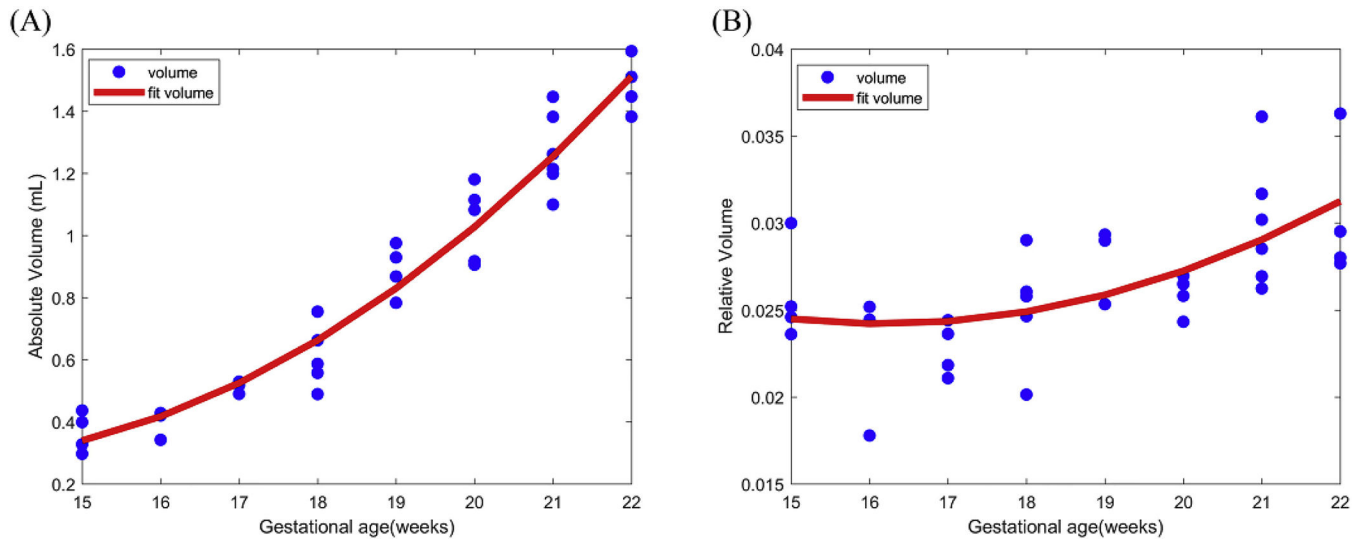
Fig. 3.
Scattergram showing the correlations between cerebellar absolute volume (A) and relative volume (B) and gestational age in weeks.
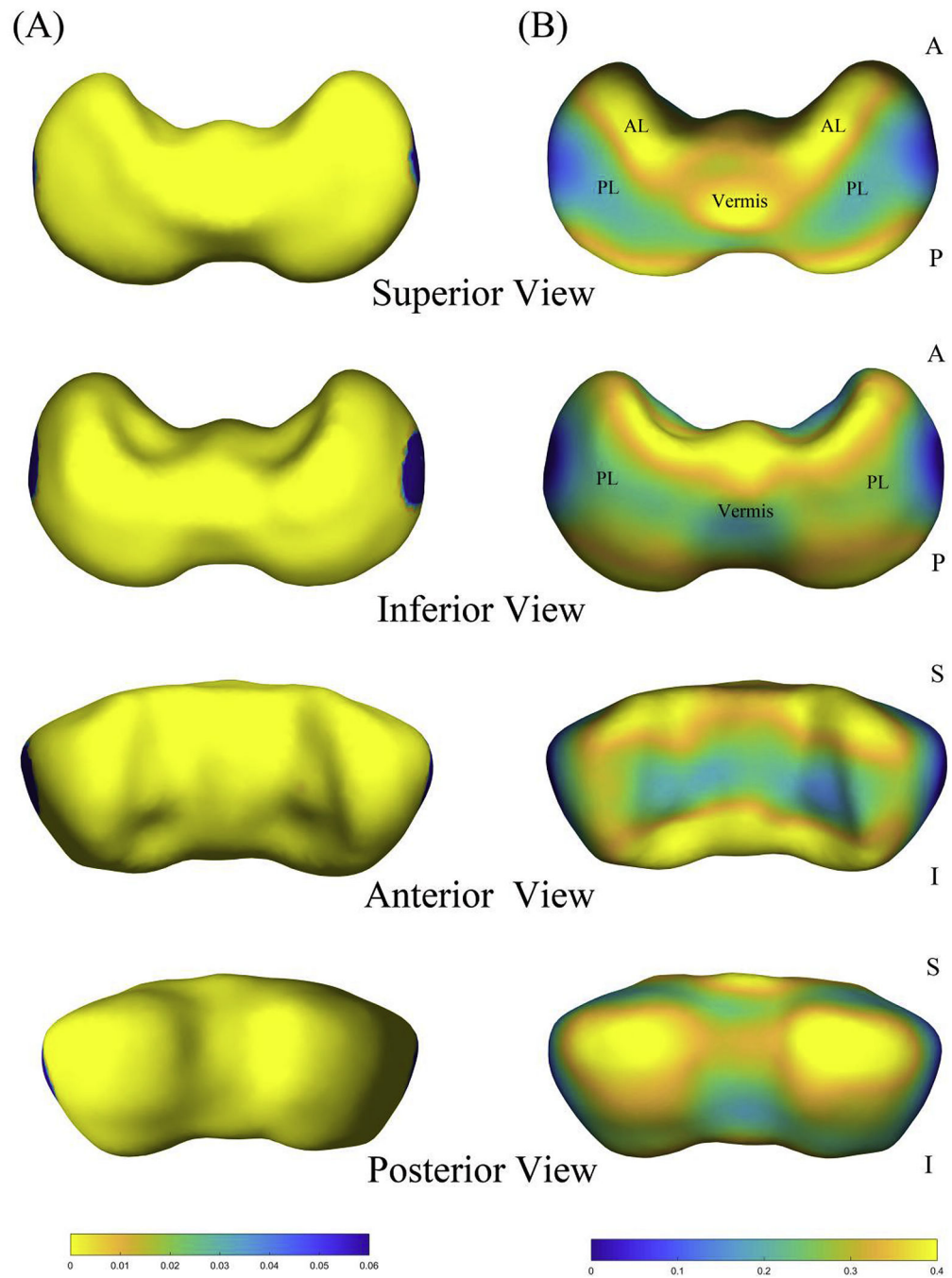
Fig. 4.
Shape analysis results of the cerebellar surface. (A) P-value map is overlaid on the template of the cerebellum. (B) Regression coefficient map of the shape statistics. Superior, inferior, anterior, and posterior views are shown. Abbreviations: (AL) anterior lobe; (PL) posterior lobe.

Table 1

Study demographics of the specimens.

Gestational week	Number (total 35)	Gender (male/female)	Termination of pregnancy	Formalin fixation time prior to scanning (days)
15	4	1/3	SA (2), TI, UNK	35, 42, 27, 51
16	3	2/1	SA (2), SIC	33, 56, 47
17	4	1/3	SA (2), SIC, UNK	25, 38, 40, 28
18	5	3/2	SA (2), TI, UNK (2)	16, 50, 29, 32, 23
19	4	2/2	SA (2), SIC (2)	43, 26, 34, 53
20	5	1/4	SA (3), SIC, UNK	27, 34, 44, 37, 50
21	6	1/5	SA (2), SIC (2), UNK (2)	42, 37, 20, 19, 23, 27
22	4	1/3	SIC (2), UNK (2)	43, 53, 24, 30

Abbreviations: TI, teratogenesis infection; SA, spontaneous abortion; SIC, stressful intrauterine conditions; UNK, unknown reasons of malformation (not brain) detected by MRI.